CRYSTAL GROWTH & DESIGN

Article

pubs.acs.org/crystal

Stepwise Synthesis of Diverse Isomer MOFs via Metal-Ion Metathesis in a Controlled Single-Crystal-to-Single-Crystal Transformation

Published as part of a Crystal Growth and Design virtual special issue on Crystal Engineering of Nanoporous Materials for Gas Storage and Separation

Zhenyu Xiao, Yutong Wang, Shiyu Zhang, Weidong Fan, Xuelian Xin, Xiaolin Pan, Liangliang Zhang,* and Daofeng Sun*

State Key Laboratory of Heavy Oil Processing, College of Science, China University of Petroleum (East China), Qingdao, Shandong 266580, People's Republic of China

Supporting Information

ABSTRACT: Two new metal−organic frameworks (MOFs) based on TMBDI linker (TMBDI = 2,3,5,6-tetramethyl-1,4-diisophthalate) and $[M_2(COO)_4]$ paddlewheel, $\{[Zn_2(TMBDI)(H_2O)_2]\bullet 2.5DMF\bullet 2(1,4\text{-dioxane})\bullet 6H_2O\}_n$ (**UPC-6**) and $\{[Co_2(TMBDI)(DMA)_2]\bullet 2DMA\bullet 5EtOH\}_n$ (**UPC-8**), have been obtained under solvothermal conditions. Due to the low stability of Zn/Co paddlewheels upon the removal of axial solvates, **UPC-6** and **UPC-8** possesses a very low surface area and adsorption capacity. Through metal-ion metathesis in a single-crystal-to-single-crystal fashion, two new Cu(II) MOFs (termed **Cu-UPC-6** and **Cu-UPC-8**) with identical robust frameworks were produced, which could not be prepared by routine solvothermal methods. Meanwhile, the influence of the reaction solvents on the metathesis process were also investigated, and the results show that the form of solvented ions can induce obviously kinetic issues. Through gas adsorption measurements, the stability and porosity of frameworks have been shown improved significantly.

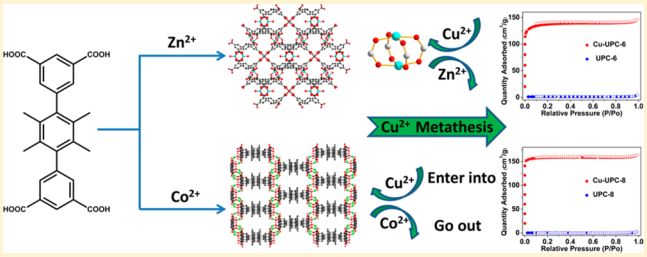

INTRODUCTION

As an emerging class of crystalline materials, metal−organic frameworks (MOFs) have attracted enormous interest in various applications, including gas storage and separation,[1−4] catalysis,[2,5−7] luminescence,[8−11] and so on.[12−16] While several MOFs with various networks and pores have been developed by the utilization of highly stable or connected secondary building units (SBUs) and rigid bridging ligands with suitable functional groups, the design and synthesis of MOF materials with diverse structures and permanent porosity remains a challenge.[17−21] Recently, the development of single-crystal-to-single-crystal (SCSC) transformation technology has made it possible to construct regioselective and robust products through ligand exchange or metal-ion metathesis.[22−25] Generally, through metal-ion metathesis process, new structures and topologies of MOFs that are inaccessible through direct solution reactions can be successfully assembled with significantly improved stability compared to the original unstable MOFs when the old, less stable SBU is replaced by a newer, more robust one.[26−28] Utilizing MOF-5 as a template, Dincă et al. realized metal-ion metathesis from Zn (II) to Ti/V/Cr (III) or V/Cr/Mn/Fe (II) through a postsynthetic ion metathesis (PSIM) strategy in 2013.[29] Following that, Zhou et al. successful obtained a series of Ti-MOFs with predesigned topologies and structures through a high valence metathesis and oxidation (HVMO) strategy in 2016.[30] Now, by quantifying the interaction of the SBU with the metal ions, the metal-ion exchange can be predicted to some extent, providing a tool for rational synthesis of new materials with specific properties.[22,31]

The paddlewheel SBU $[M_2(COO)_4]$ (M = Cu^{2+}, Zn^{2+}, Ni^{2+}, and Co^{2+}) is the most well-known cluster among the reported metal carboxylate MOFs, where the axial locations are dominated by N-donor auxiliary ligands or solvent molecules.[32−34] Among them, Cu-paddlewheel shows the best stability and are often combined with polyaromatic carboxylate linkers containing isophthalate moieties to construct permanent porous frameworks with excellent gas molecule storage capacities.[35,36] For example, three new MOFs (named **SDU-6**, **-7**, **-8**) reported by our group have been successfully prepared from C_3-symmetric carboxylate-linkers with different functional groups (hydroxyl, methyl, and isobutyl) and Cu-paddlewheel SBUs, showing high BET surface areas of 2826, 2713, and 2516 $m^2\ g^{-1}$, respectively, after evacuation at 80 °C overnight.[37] Although different functional groups were incorporated in their networks, they are all constructed by packing of similar nanosized cages and show a unified *rht*-topology. Similar phenomena have been commonly reported

Received: January 24, 2017
Revised: March 7, 2017
Published: March 10, 2017

DOI: 10.1021/acs.cgd.7b00118
Cryst. Growth Des. 2017, 17, 4084−4089

that the decoration of the bridging ligands is not an effective way to produce Cu-paddlewheel based MOFs with diverse topologies and pore structures, such as **NOTT-101**, **-105**, **-106**, **-107**, **-108**, and **PCN-14**. Those MOFs all demonstrated a *NbO*-type network, although their linkers are decorated with different functional groups.[38] Meanwhile, the construction of unique MOF networks based on one given ligand and Cu-paddlewheel has also been proved to be an unwise way for a thermodynamic stability framework has always been obtained.[39] Those two habits of Cu-paddlewheel based MOFs are great obstacle for the target to get diverse topology network and pore feature.

We are interested in the construction of diverse pore Cu-paddlewheel MOF networks based on organic carboxylate linkers. In this work, a four carboxylate ligand which has produced two Cu-paddlewheel MOFs with different networks (**NOTT-107** possesses an *NbO*-type network and **NPC-4** possesses a *ssb*-type network) was selected as a linker, and the relevant complexes $\{[Zn_2(TMBDI)(H_2O)_2]\bullet 2.5DMF\bullet 2(1,4\text{-dioxane})\bullet 6H_2O\}_n$ (**UPC-6**) based on a Zn-paddlewheel and $\{[Co_2(TMBDI)\ (DMA)_2]\bullet 2DMA\bullet 5EtOH\}_n$ (**UPC-8**) based on a Co-paddlewheel were synthesized (TMBDI = 2,3,5,6-tetramethyl-1,4-diisophthalate). On the basis of our previous work on metal metathesis,[40] **UPC-6** (*hyw*-type network) and **UPC-8** (*lvt*-type network) can be turned into **Cu-UPC-6** and **Cu-UPC-8** by the SCSC transformation of replacing Zn/Co(II) ions with Cu(II) ions in their paddlewheel units. In this way, two new isomers of Cu-paddlewheel and TMBDI based MOFs have been successfully obtained and the metal-ion metathesis strategy noticeably improves the stability of their frameworks.

EXPERIMENTAL SECTION

Synthesis of UPC-6, UPC-8, Cu-UPC-6, and Cu-UPC-8. *2.1. Synthesis of **UPC-6**.* H_4TMBDI (2 mg, 0.0043 mmol) and $Zn(NO_3)_2\bullet 6H_2O$ (10.1 mg, 0.034 mmol) were dissolved in DMF:1,4-dioxane:H_2O (1 mL, V:V:V = 5:2:1). The resulting colorless solution was sealed in a glass tube and heated to 90 °C over 5 h, kept for 50 h, then slowly cooled to 30 °C over 10 h. The colorless crystals were collected, washed with DMF, and dried in the air (yield: 55%, based on ligand). Elemental Analysis Calcd (%) for $\{[Zn_2(TMBDI)(H_2O)_2]\bullet 2.5DMF\bullet 2(1,4\text{-dioxane})\bullet 6H_2O\}_n$: C 45.67, H 6.19, N 3.2. Found: C 46.23, H 5.97, N 3.07. IR data (KBr, cm^{-1}): 3432 (w), 1645 (m), 1565 (s), 1450 (m), 1368 (s), 1340 (s), 1025 (w), 805 (s), 775 (w), 720 (w), 668 (w).

*2.2. Synthesis of **UPC-8**.* A mixture of $Co(NO_3)_2\bullet 6H_2O$ (25 mg, 0.086 mmol) and H_4TMBDI (15 mg, 0.032 mmol) were dissolved in 4 mL of mixed solvents (DMA/EtOH, v/v = 3:1). Then the solution was sealed in a pressure-resistant glass tube, slowly heated to 120 °C over 2 h, kept at 120 °C for 12 h, and then slowly cooled to 30 °C over 5 h. The dark-green crystals were collected by filtration and washed with fresh mother liquid (yield: 83%, based on ligand). Elemental Analysis Calcd (%) for $\{[Co_2(TMBDI)\ (DMA)_2]\bullet 2DMA\bullet 5EtOH\}_n$: C 54.07, H 7.28, N 4.85. Found: C 53.27, H 6.89, N 4.73. IR data (KBr, cm^{-1}): 3442 (m), 2928 (w), 1625 (s), 1434(m), 1378 (s), 1253 (w), 1004 (w), 803 (w), 780 (w), 727 (m), 679(w).

*2.3. Procedure for Ion Exchange for **Cu-UPC-6**.* In the ion exchange experiment, the as-synthesized crystal **UPC-6** was soaked in a $Cu(NO_3)_2/CH_3OH$ solution (10 mL, 40 g/L) for 7 days. During the period, the solution was replaced with a fresh solution of $Cu(NO_3)_2$ twice a day. This procedure was repeated, and the color of the crystals turned from colorless to blue, indicating that the metal metathesis of Zn(II) metal centers to Cu(II) has occurred. After removing the solution, the ion-exchanged crystals were washed with CH_3OH several times to remove any excess metal salt.

*2.4. Procedure for Ion Exchange for **Cu-UPC-8**.* Similar to the process of synthesis of **Cu-UPC-6**, **UPC-8** was soaked in a DMA/CH_3OH (v:v = 1:1) solution of $Cu(NO_3)_2$. Fortunately, the **Cu-UPC-8** sample can be obtained after 30 days and analyzed using single-crystal X-ray diffraction.

RESULTS AND DISCUSSION

3.1. Description of Crystal Structure. Single-crystal X-ray diffraction studies reveal that **UPC-6** crystallizes in a Tetragonal space group *P42/nnm* and is a 3D porous framework based on $Zn_2(COO)_4$ paddlewheel **SBUs**. The asymmetric unit consists of two halves Zn(II) ions, a half $TMBDI^{4-}$ ligand, and two halves coordinated water molecular. Adjacent Zn1 or Zn2 atoms are connected by four carboxyl groups to generate the slightly distorted $[Zn_2(COO)_4]$ unit with the $Zn-O_{carboxyl}$ bond length in the range of 1.982−2.128 Å and Zn1···Zn1 separation of 2.972 Å or Zn2···Zn2 separation of 2.964 Å (as shown in Figure 1b). Compared with the reported Cu-paddlewheel MOF

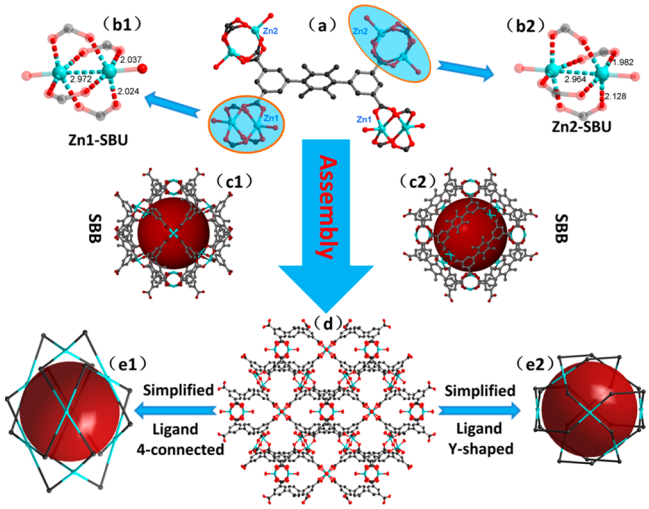

Figure 1. (a) The coordination mode of the $TMBDI^{4+}$ ligand in **UPC-6**. (b1,b2) Coordination situation of two kinds of $Zn_2(COO)_4$ paddlewheels in **UPC-6**. (c1,c2) The supermolecular building blocks (**SBB**) viewed from different direction. (d) Projection view of 3D open framework along the *b*-axis. (e1,e2) The topological nets when the $TMBDI^{4+}$ ligand was simplified to different connected nodes.

based on the same ligand, **NPC-4** has a $Cu-O_{carboxyl}$ bond length of 1.960 Å and a Cu···Cu distance of 2.666 Å, which indicates the lower stability of $[Zn_2(COO)_4]$ SBUs. Furthermore, the SBUs are linked by the backbone of four-connected H_4TMBDI ligands to form a supermolecular building block (**SBB**) with large cavities (Figure 1c), which were further packed into a complicated three-dimensional (3D) framework (see Figure 1d). PLATON program analysis of **UPC-6** demonstrates that there is ∼62.94% solvent-accessible volume (6347.2/10084.8 $Å^3$). Interestingly, the network of **UPC-6** clearly differs from **NOTT-107** and **NPC-4**, although they all based on H_4TMBDI ligand and similar paddlewheel SBUs. To further study the structure differences, the topology of **UPC-6** was analyzed using TOPOS. If the ligand was viewed as a four-connected linker, the *hyw* topology type would be expected (Figure 1e1). The network was different from *NbO* type (**PCN-14**), *PtS* type (**NOTT-109**), or *ssb* type (**NPC-4**),[41] which is commonly adopted by most MOFs constructed from four-connected ligands and SBUs. By simplifying the bridging ligands as double Y-shaped linkers and the paddlewheel SBUs

DOI: 10.1021/acs.cgd.7b00118
Cryst. Growth Des. 2017, 17, 4084−4089

as 4-connected nodes, the structure of **UPC-6** can be simplified into a *hyx* network (Figure 1e2).

When Co^{2+} ions were used, a novel 3D network (named **UPC-8**) based on Co-paddlewheel was successful constructed, which crystallizes in a Cubic space group *Imcm*. The asymmetric unit of **UPC-8** consists of a half of Co(II) ion, one-quarter of carboxylate ligand, and a half of coordinated DMA molecule. Two crystallographically equivalent Co atoms are bridged by four carboxyl groups to obtain an uncommon $Co_2(COO)_4$ paddlewheel SBU. In this SBU, the $Co1-O1_{carboxyl}$ and $Co1-O2_{carboxyl}$ bonds length are 1.995 and 2.047 Å (as shown in Figure 2c1), respectively, which attribute to a higher

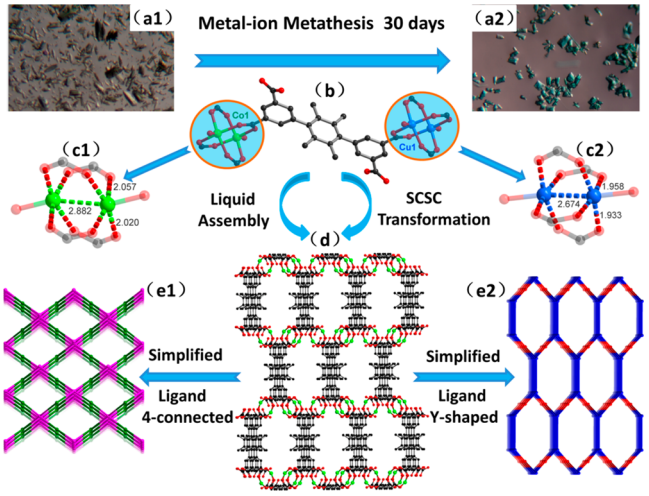

Figure 2. (a1,a2) Photographs of the **UPC-8** sample before and after the metal-ion metathesis. (b) The coordination mode of the $TMBDI^{4+}$ ligand in **UPC-8** network. (c1,c2) Coordination situation of $Co_2(COO)_4$ paddlewheel in **UPC-8** or $Cu_2(COO)_4$ paddlewheel in **Cu-UPC-8**, respectively. (d) Projection view of 3D open framework along the *a*-axis. (e1,e2) The topological nets when the TMBDI ligand was simplified to different connected nodes.

degree of distortion of the Co-paddlewheel than the Zn-paddlewheel in **UPC-6** (Figure 1c). The $Co1-O3_{DMA}$ bond length is 1.989 Å and the Co1···Co1 separation distance is 2.900 Å. The interlinkage between Co-paddlewheels and four-connected tetra-carboxylate ligands generates the final 3D framework structure with 1D narrow rectangular channels with side length of ~7 × 10 Å (Figure 2d). The PLATON analysis of **UPC-8** demonstrates that the solvent-accessible volume is 2913.5 $Å^3$ (~63.81% of total volume), which is bigger than the value of **UPC-6** and **NPC-4** (~60.80%). Then, topology analysis was also employed to identify the difference between these networks. When the Co-paddlewheel and TMBDI ligand were simplified as four-connected nodes, a novel *lvt* topology type would be expected (Figure 2-e1), which was different from **UPC-6** and other reported MOFs constructed from four-connected ligands and paddlewheel SBUs. By simplifying the bridging ligands as double Y-shaped linkers and the paddlewheel SBUs as four-connected nodes, the structure of **UPC-8** can be simplified into a *lil* network (Figure 2e2). The whole framework can be viewed as the square crossing of two groups honeycomb 2-D networks which parallel to each other in every group with the distance 14.78 Å between two adjacent parallel 2-D nets.

After the Cu-ion metathesis process in a DMA/CH_3OH solution (v:v = 1:1), we obtained the single-crystal **Cu-UPC-8** sample suitable for single-crystal X-ray diffraction analysis. Large solvent-accessible volumes were occupied by disordered solvent molecules and no satisfactory model could be achieved, so the SQUEEZE routine was used to remove these electron densities. The structure was refined by the new .HKL file, and the crystal quality does not show obvious changes (as shown in Supporting Information, Table S1). **Cu-UPC-8** keeps the same *lvt* topology of **UPC-8** network, but the crystal space group shows a slight difference, changing from *Imcm* to *Imma*. In the new Cu-based framework, the paddlewheel unit demonstrate a lower distorted degree, with the separation of Cu1···Cu1 of 2.679 Å, the $Cu1-O1_{carboxyl}$ and $Cu1-O2_{carboxyl}$ of 1.933 and 1.958 Å, respectively.

3.2. Study of Controlled Single-Crystal-to-Single-Crystal Metal Metathesis Process. Zinc/cobalt paddlewheel metal−organic frameworks (MOFs) frequently exhibit low stability or complete collapse upon the removal of axial ligands, and there are very few examples were reported on gas adsorption of those MOFs in former studies. To improve the network stability, metal metathesis process was subjected by us to construct Cu-paddlewheel SBUs, which is a commonly stable one according to previous reported.

First, **UPC-6** and **UPC-8** were treated by metathesis through the conventional method of soaking in $Cu(NO_3)_2/DMF$ solution (40 g/L). However, the metathesis process almost did not occur and the exchange fraction of Zn/Co centers that were substituted by Cu^{2+} ions is below 4.3% and 12.6%, respectively, even after one month according to the results of ICP. To improve the efficiency of the metal metathesis process, different solvents were employed. After subjecting **UCP-6** and **UPC-8** to suitable solvents system at room temperature ($CH_3OH$and DMF:CH_3OH = 1:1 v/v, respectively), the color of the original single-crystal samples changed from colorless/dark-green to blue (the MOFs after metathesis are termed **Cu-UPC-6** and **Cu-UPC-8**, respectively). This metal metathesis process was proved to be a single-crystal-to-single-crystal transformation process by power X-ray diffraction. The similarities of the IR spectra confirm the same ligand and similar organic groups in these compounds (see the IR spectra in Supporting Information, Figure S4 and Figure S5). Then, the new crystal data of **Cu-UPC-8** has been obtained by single-crystal X-ray diffraction, but the attempt to determine the crystal structure of **Cu-UPC-6** has proved to be unsuccessful owing to cracks on the crystals. As shown in Supporting Information, Table S1, the goodness of fit value of **Cu-UPC-8** crystal parameters after metal metathesis is better than **UPC-8**, which may owe to the enhanced stability of Cu-paddlewheel SBUs in the MOF framework. ICP test was utilized to check the ratio of Zn/Co metal centers replaced by Cu(II) ions in total. The results suggest that metal metathesis was nearly completed, and only 2% Zn metal centers or 4% Co metal centers were left in the skeleton. In this way, four different networks (**Cu-UPC-6**, **Cu-UPC-8**, **NOTT-107**, and **NPC-4**) can be constructed by the same ligand and Cu-paddlewheel SBU, but their framework and pore structures are quite unique. Compared to the pore cavity in **Cu-UPC-6**, **NOTT-107**, and **NPC-4** with different pore sizes, **Cu-UPC-8** is comprised of a 1D connected pore along the *a*-axis. Meanwhile, the products of direct synthesis, **Cu-UPC-6** and **Cu-UPC-8**, using Cu^{2+} salts and the TMBDI ligand have been proved unsuccessful, as **NPC-4**, **NOTT-107**, or other low crystallinity powders were always obtained (as shown in Supporting Information, Figure S3). Therefore, four isomer MOFs were produced by

DOI: 10.1021/acs.cgd.7b00118
Cryst. Growth Des. 2017, 17, 4084−4089

controlled a single-crystal-to-single-crystal metal metathesis process.

There are many factors that affect the single-crystal-to-single-crystal metal metathesis process, such as the types of metal ions, the characteristics of metal coordination spheres, the environments of the pore structures, and metal metathesis conditions (reaction time, reaction temperature, and concentration of ions in solvent). To unveil the influence of solvent, first, we subjected as-synthesized crystal samples to metal metathesis with different Cu^{2+} solvents (DMF, DMF:CH_3OH = 1:1 and CH_3OH) while keeping the other conditions identical. After three days, the fraction of Co^{2+} metal centers exchanged by Cu^{2+} ions in **UPC-8** is about 99% for CH_3OH, 12% for DMF:CH_3OH, and 1% for DMF. Though **UPC-8** shows the fastest ions exchange efficiency in CH_3OH, the morphology of **UPC-8** could not be maintained. So the solution of DMF:CH_3OH was ultimately selected to synthesize suitable single-crystal samples. For **UPC-6**, CH_3OH also showed the fastest metathesis with 53% Zn^{2+} centers exchanged by Cu^{2+} after three days, while the DMF and DMF:CH_3OH = 1:1 solution did not show evidence of metathesis. These results indicated that the diffusion of metal ions into the channels might be very sensitive to the size of the solvated metal ion and the pore structure of the framework. Such a SCSC transmetalation process is irreversible, i.e., Cu(II) ions in daughter structures cannot be replaced by Zn(II) ions even in a concentrated CH_3OH solution containing $Zn(NO_3)_2$ (40 g/L) under long exchange time (1 month). The fact suggests that the frameworks of **Cu-UPC-6** and **Cu-UPC-8** are thermodynamically more stable than parent crystals, which is in agreement with the Irving–Williams series of the stability in the order Co < Zn < Cu.

3.3. Gas Adsorption of UPC-6, Cu-UPC-6, UPC-8, and Cu-UPC-8. To compare the stability and the porosity of the complexes before and after the metal-ion metathesis process, gas-uptake measurements for desolvated samples were performed. Before the measurement, the freshly synthesized and exchanged crystal samples of **UPC-6**, **Cu-UPC-6**, **UPC-8**, and **Cu-UPC-8** were immersed in methanol to exchange the less-volatile solvates. Then evacuation was done under a dynamic vacuum at 60 °C for 3 h to yield the activated samples. The PXRD patterns of active samples are shown in Supporting Information, Figures S1 and S2, which indicates that the metathesis process will dramatically improve the robustness of the framework.

As shown in Figure 3, **Cu-UPC-6** and **Cu-UPC-8** all exhibit typical type-I isotherms for N_2 at 77 K, suggesting the retention of stable microporous structures after the metal-ion metathesis process of crystalline samples. **Cu-UPC-6** can adsorb 146 cm^3 g^{-1} of N_2 molecules under the conditions of 77 K and 1 atm, which is almost 31.4 times greater than that of **UPC-6** (4.65 cm^3 g^{-1}). For **UPC-8** and **Cu-UPC-8**, the capacities of adsorption were improved from 2.72 to 164.2 cm^3 g^{-1}, which increased about 60.4 times after the metathesis process. These results indicate that the metal-ion metathesis significantly increases the stability and preserves the porosity of the framework. The Langmuir surface area determined by the N_2 isotherms, are 598.3 m^2 g^{-1} for **Cu-UPC-6** and 689.7 m^2 g^{-1} for **Cu-UPC-8**, which represents 13120% and 45078% increases, compared to that of **UPC-6** (langmuir: 4.56 m^2 g^{-1}) and **UPC-8** (langemuir: 1.53 m^2 g^{-1}).

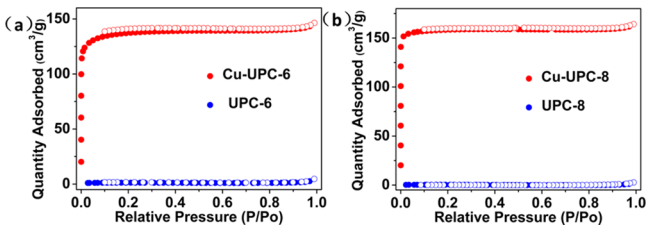

Figure 3. (a) N_2 sorption isotherms at 77 K for **UPC-6** and **Cu-UPC-6**. (b) N_2 sorption isotherms at 77 K for **UPC-8** and **Cu-UPC-8**.

Low-pressure H_2, CO_2, and CH_4 uptakes of activated samples were continuously monitored using volumetric gas adsorption measurements. As shown in Figure 4, the activated

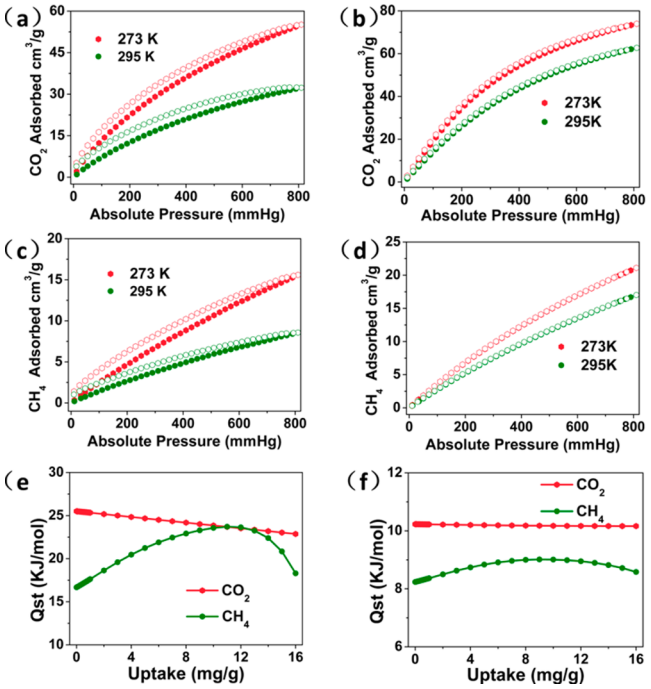

Figure 4. (a,c) CO_2 and CH_4 sorption isotherms for **Cu-UPC-6** at 273 and 295 K. (b,d) CO_2 and CH_4 sorption isotherms for **Cu-UPC-8** at 273 and 295 K. (e) The CO_2 and CH_4 Q_{st} of **Cu-UPC-6**. (f) The CO_2 and CH_4 Q_{st} of **Cu-UPC-8**.

Cu-UPC-6 and **Cu-UPC-8** exhibit classical reversible type I isotherms for CH_4 and CO_2. The uptakes of CO_2 are 74 cm^3 g^{-1} at 273 K and 62.7 cm^3 g^{-1} at 295 K for **Cu-UPC-8**, which are much higher than those of **Cu-UPC-6** (55.1 and 32.3 cm^3 g^{-1}, at 273 and 295 K). Under similar conditions at 273 and 295 K, the CH_4 adsorption capacities of active **Cu-UPC-8** are also higher than **Cu-UPC-6**. The two complexes contain the same unsaturated Cu-paddlewheel SBUs and π-electrons of organic ligand, but they possess different pore features: a cage pore for **Cu-UPC-6** and a 1D connected pore for **Cu-UPC-8**. So the most possibe reason for the unique adsorption performance may attributed to the steric hindrance of different pores. To further analyze this effect, the isosteric adsorption enthalpies (Q_{st}) was calculated from the Clausius–Clapeyron equation. As shown in Figure 4e, the Q_{st} plots of CO_2 and CH_4 on **Cu-UPC-6** lie in the range of 25.5–22.8 and 23.7–16.6 kJ mol^{-1}, higher than the average values for **Cu-UPC-8** of 10.2 and 8.5 kJ mol^{-1} (Figure 4f), respectively. Though the Q_{st} values of **Cu-UPC-6** for CO_2 and CH_4 is about 2.5 times that of **Cu-UPC-8**, the adsorption capacities are inferior to **Cu-UPC-8**.

DOI: 10.1021/acs.cgd.7b00118
Cryst. Growth Des. 2017, 17, 4084–4089

The phenomenon may suggest that pore feature is the primary determinant of adsorption performance for the two isomer MOFs. The stronger binding strength between the **Cu-UPC-8** framework and gas molecules may be attributed to their constricted pore features, which were also observed by our and other reported works that the constricted pores will possess higher Q_{st} values.[20,21,39] The Q_{st} of CH_4 on **Cu-UPC-6** is comparable to the reported Cu-paddlewheel based cage pore MOFs, such as **ZJU-199** (19 kJ mol^{-1})[42] and **MFM-130** (16 kJ mol^{-1}),[43] indicating that the framework of **Cu-UPC-6** exhibits high affinity to CH_4 molecules.

CONCLUSIONS

The construction of MOFs composed of Cu-paddlewheel SBUs and identical organic ligands with unique topologies and pores is an attractive target for chemists because thermodynamically stable networks are always obtained. In the present work, two new MOFs based on Zn/Co-paddlewheels and H_4BDMI were successful synthesized. Compared with reported MOFs (NPC-4) constructed by Cu-paddlewheel and H_4BDMI, the two new networks show different pores and topologies. The gas adsorptions of **UPC-6** and **UPC-8** have been measured for the first time, but they all show low adsorption performances due to the instability of their networks when solvents are removed from the axial of Zn/Co paddlewheels. Then, a metal-ion metathesis process was applied to improve the porosity and stability, and two daughter structures with Cu(II) metal centers were produced. These daughter structures show higher adsorption performances compared to their parent networks. In this two-step synthesis strategy, four MOF isomers with different pores and topologies were obtained. The study of the metal metathesis process demonstrated that the solvents and pore structure are important factors for controlling the reaction efficiency. Our research results provide a new way to build isomer MOF structures based on Cu-paddlewheel and further confirmed the important role of metal-ion metathesis for improving the stability and permanent porosity.

ASSOCIATED CONTENT

Supporting Information

The Supporting Information is available free of charge on the ACS Publications website at DOI: 10.1021/acs.cgd.7b00118.

Full details for experimental procedures, single-crystal structure determination, syntheses of the organic linker H_4TMBDI, PXRD, FT-IR, and TGA data (PDF)

Accession Codes

CCDC 1522208−1522210 contains the supplementary crystallographic data for this paper. These data can be obtained free of charge via www.ccdc.cam.ac.uk/data_request/cif, or by emailing data_request@ccdc.cam.ac.uk, or by contacting The Cambridge Crystallographic Data Centre, 12, Union Road, Cambridge CB2 1EZ, UK; fax: +44 1223 336033.

AUTHOR INFORMATION

Corresponding Authors

*For D.S.: phone, 86 532 86983208; fax, 86 532-86983208; E-mail: dfsun@upc.edu.cn.

*For L.Z.: E-mail: liangliangzhang@upc.edu.cn.

ORCID

Daofeng Sun: 0000-0003-3184-1841

Notes

The authors declare no competing financial interest.

ACKNOWLEDGMENTS

This work was supported by National Natural Science Foundation of China (no. 21571187), NCET-11-0309, Taishan Scholar Foundation (ts201511019).

REFERENCES

(1) Ma, S.; Sun, D.; Ambrogio, M.; Fillinger, J. A.; Parkin, S.; Zhou, H. *J. Am. Chem. Soc.* **2007**, *129* (7), 1858−1859.

(2) Xu, H.; Hu, J.; Wang, D.; Li, Z.; Zhang, Q.; Luo, Y.; Yu, S.; Jiang, H. *J. Am. Chem. Soc.* **2015**, *137* (42), 13440−13443.

(3) Chen, Y.; Liu, Y.; Liu, D.; Bosch, M.; Zhou, H. *J. Am. Chem. Soc.* **2015**, *137*, 2919−2930.

(4) Murray, L. J.; Dinca, M.; Yano, J.; Chavan, S.; Bordiga, S.; Brown, C. M.; Long, J. R. *J. Am. Chem. Soc.* **2010**, *132* (23), 7856−7857.

(5) McGuirk, C. M.; Katz, M. J.; Stern, C. L.; Sarjeant, A. A.; Hupp, J. T.; Farha, O. K.; Mirkin, C. A. *J. Am. Chem. Soc.* **2015**, *137* (2), 919−925.

(6) Li, B.; Leng, K.; Zhang, Y.; Dynes, J. J.; Wang, J.; Hu, Y.; Ma, D.; Shi, Z.; Zhu, L.; Zhang, D.; Sun, Y.; Chrzanowski, M.; Ma, S. *J. Am. Chem. Soc.* **2015**, *137* (12), 4243−4248.

(7) Horike, S.; Dincă, M.; Tamaki, K.; Long, J. R. *J. Am. Chem. Soc.* **2008**, *130* (18), 5854−5855.

(8) Seth, S.; Savitha, G.; Jhulki, S.; Moorthy, J. N. *Cryst. Growth Des.* **2016**, *16* (4), 2024−2032.

(9) White, K. A.; Chengelis, D. A.; Gogick, K. A.; Stehman, J.; Rosi, N. L.; Petoud, S. *J. Am. Chem. Soc.* **2009**, *131* (50), 18069−18071.

(10) Wang, W.; Yang, J.; Wang, R.; Zhang, L.; Yu, J.; Sun, D. *Cryst. Growth Des.* **2015**, *15* (6), 2589−2592.

(11) Wang, W.; Yang, J.; Wang, R.; Zhang, L.; Yu, J.; Sun, D. *Cryst. Growth Des.* **2015**, *15* (6), 2589−2592.

(12) Kang, Y.; Liu, X.; Yan, N.; Jiang, Y.; Liu, X.; Sun, L.; Li, J. *J. Am. Chem. Soc.* **2016**, *138* (19), 6099−6102.

(13) Zhang, Y.; Furukawa, H.; Ko, N.; Nie, W.; Park, H. J.; Okajima, S.; Cordova, K. E.; Deng, H.; Kim, J.; Yaghi, O. M. *J. Am. Chem. Soc.* **2015**, *137* (7), 2641−2650.

(14) Lu, W.; Wei, Z.; Gu, Z.; Liu, T.; Park, J.; Park, J.; Tian, J.; Zhang, M.; Zhang, Q.; Gentle, T., III; Bosch, M.; Zhou, H. *Chem. Soc. Rev.* **2014**, *43*, 5561−5593.

(15) Deng, H.; Olson, M. A.; Stoddart, J. F.; Yaghi, O. M. *Nat. Chem.* **2010**, *2* (6), 439−443.

(16) Feng, D.; Wang, K.; Su, J.; Liu, T.; Park, J.; Wei, Z.; Bosch, M.; Yakovenko, A.; Zou, X.; Zhou, H. *Angew. Chem., Int. Ed.* **2015**, *54* (1), 149−154.

(17) Li, M.; Li, D.; O'Keeffe, M.; Yaghi, O. M. *Chem. Rev.* **2014**, *114*, 1343−1370.

(18) Liu, C.; Ding, Y.; Shi, X.; Zhang, D.; Hu, M.; Yin, Y.; Li, D. *Cryst. Growth Des.* **2009**, *9* (3), 1275−1277.

(19) Xue, M.; Ma, S.; Jin, Z.; Schaffino, R. M.; Zhu, G.; Lobkovsky, E. B.; Qiu, S.; Chen, B. *Inorg. Chem.* **2008**, *47* (15), 6825−6828.

(20) Zhao, X.; Liu, F.; Zhang, L.; Sun, D.; Wang, R.; Ju, Z.; Yuan, D.; Sun, D. *Chem. - Eur. J.* **2014**, *20* (3), 649−652.

(21) Wang, R.; Meng, Q.; Zhang, L.; Wang, H.; Dai, F.; Guo, W.; Zhao, L.; Sun, D. *Chem. Commun.* **2014**, *50* (38), 4911−4914.

(22) Brozek, C. K.; Dinca, M. *Chem. Soc. Rev.* **2014**, *43* (16), 5456−67.

(23) Kim, M.; Cahill, J. F.; Fei, H.; Prather, K. A.; Cohen, S. M. *J. Am. Chem. Soc.* **2012**, *134* (43), 18082−18088.

(24) Liu, M.; Bi, Y.; Dang, Q.; Zhang, X. *Dalton Trans.* **2015**, *44* (46), 19796−19799.

(25) Park, J.; Feng, D.; Zhou, H. *J. Am. Chem. Soc.* **2015**, *137* (4), 1663−1672.

(26) Wang, X. J.; Li, P. Z.; Liu, L.; Zhang, Q.; Borah, P.; Wong, J. D.; Chan, X. X.; Rakesh, G.; Li, Y.; Zhao, Y. *Chem. Commun. (Cambridge, U. K.)* **2012**, *48* (83), 10286−8.

(27) Song, X.; Kim, T. K.; Kim, H.; Kim, D.; Jeong, S.; Moon, H. R.; Lah, M. S. *Chem. Mater.* **2012**, *24* (15), 3065−3073.
(28) Liu, T.; Zou, L.; Feng, D.; Chen, Y.; Fordham, S.; Wang, X.; Liu, Y.; Zhou, H. *J. Am. Chem. Soc.* **2014**, *136* (22), 7813−7816.
(29) Brozek, C.; Dincă, M. *J. Am. Chem. Soc.* **2013**, *135*, 12886−12891.
(30) Zou, L.; Feng, D.; Liu, T.; Chen, Y.; Yuan, S.; Wang, K.; Wang, X.; Fordham, S.; Zhou, H.-C. *Chem. Sci.* **2016**, *7*, 1063−1069.
(31) Wei, Z.; Lu, W.; Jiang, H.; Zhou, H. *Inorg. Chem.* **2013**, *52* (3), 1164−1166.
(32) Li, L.; Bell, J. G.; Tang, S.; Lv, X.; Wang, C.; Xing, Y.; Zhao, X.; Thomas, K. M. *Chem. Mater.* **2014**, *26* (16), 4679−4695.
(33) Wen, H.; Wang, H.; Li, B.; Cui, Y.; Wang, H.; Qian, G.; Chen, B. *Inorg. Chem.* **2016**, *55* (15), 7214−7218.
(34) Farha, O. K.; Eryazici, I.; Jeong, N. C.; Hauser, B. G.; Wilmer, C. E.; Sarjeant, A. A.; Snurr, R. Q.; Nguyen, S. T.; Yazaydın, A. Ö.; Hupp, J. T. *J. Am. Chem. Soc.* **2012**, *134* (36), 15016−15021.
(35) Yan, Y.; Blake, A. J.; Lewis, W.; Barnett, S. A.; Dailly, A.; Champness, N. R.; Schröder, M. *Chem. - Eur. J.* **2011**, *17* (40), 11162−11170.
(36) Wang, Y.; Ye, G.; Chen, H.; Hu, X.; Niu, Z.; Ma, S. *J. Mater. Chem. A* **2015**, *3* (3), 15292−15298.
(37) Zhao, X.; Sun, D.; Yuan, S.; Feng, S.; Cao, R.; Yuan, D.; Wang, S.; Dou, J.; Sun, D. *Inorg. Chem.* **2012**, *51* (19), 10350−10355.
(38) Lin, X.; Telepeni, I.; Blake, A. J.; Dailly, A.; Brown, C. M.; Simmons, J. M.; Zoppi, M.; Walker, G. S.; Thomas, K. M.; Mays, T. J.; Hubberstey, P.; Champness, N. R.; Schröder, M. *J. Am. Chem. Soc.* **2009**, *131* (6), 2159−2171.
(39) Li, L.; Xue, H.; Wang, Y.; Zhao, P.; Zhu, D.; Jiang, M.; Zhao, X. *ACS Appl. Mater. Interfaces* **2015**, *7* (45), 25402−25412.
(40) Yang, J.; Wang, X.; Dai, F.; Zhang, L.; Wang, R.; Sun, D. *Inorg. Chem.* **2014**, *53* (19), 10649−10653.
(41) Ma, S.; Sun, D.; Simmons, J. M.; Collier, C. D.; Yuan, D.; Zhou, H. *J. Am. Chem. Soc.* **2008**, *130* (3), 1012−1016.
(42) Zhang, L.; Zou, C.; Zhao, M.; Jiang, K.; Lin, R.; He, Y.; Wu, C.; Cui, Y.; Chen, B.; Qian, G. *Cryst. Growth Des.* **2016**, *16* (12), 7194−7197.
(43) Yan, Y.; Juríček, M.; Coudert, F.; Vermeulen, N. A.; Grunder, S.; Dailly, A.; Lewis, W.; Blake, A. J.; Stoddart, J. F.; Schröder, M. *J. Am. Chem. Soc.* **2016**, *138* (10), 3371−3381.

DOI: 10.1021/acs.cgd.7b00118
Cryst. Growth Des. 2017, 17, 4084−4089